Unexpected Sensitivity of sst_2 Antagonists to N-Terminal Radiometal Modifications

Melpomeni Fani[1], Friederike Braun[1], Beatrice Waser[2], Karin Beetschen[2], Renzo Cescato[2], Judit Erchegyi[3], Jean E. Rivier[3], Wolfgang A. Weber[1], Helmut R. Maecke[1], and Jean Claude Reubi[2]

[1]Department of Nuclear Medicine, University Hospital Freiburg, Freiburg, Germany; [2]Division of Cell Biology and Experimental Cancer Research, Institute of Pathology, University of Berne, Berne, Switzerland; and [3]Clayton Foundation Laboratories for Peptide Biology, Salk Institute for Biological Studies, La Jolla, California

Chelated somatostatin agonists have been shown to be sensitive to N-terminal radiometal modifications, with Ga-DOTA agonists having significantly higher binding affinity than their Lu-, In-, and Y-DOTA correlates. Recently, somatostatin antagonists have been successfully developed as alternative tracers to agonists. The aim of this study was to evaluate whether chelated somatostatin antagonists are also sensitive to radiometal modifications and how. We have synthesized 3 different somatostatin antagonists, DOTA-*p*-NO_2-Phe-c[D-Cys-Tyr-D-Aph(Cbm)-Lys-Thr-Cys]-D-Tyr-NH_2, DOTA-Cpa-c[D-Cys-Aph(Hor)-D-Aph(Cbm)-Lys-Thr-Cys]-D-Tyr-NH_2 (DOTA-JR11), and DOTA-*p*-Cl-Phe-c[D-Cys-Tyr-D-Aph(Cbm)-Lys-Thr-Cys]-D-Tyr-NH_2, and added various radiometals including In(III), Y(III), Lu(III), Cu(II), and Ga(III). We also replaced DOTA with 1,4,7-triazacyclononane,1-glutaric acid-4,7-acetic acid (NODAGA) and added Ga(III). The binding affinity of somatostatin receptors 1 through 5 was evaluated in all cases. In all 3 resulting antagonists, the Ga-DOTA analogs were the lowest-affinity radioligands, with a somatostatin receptor 2 binding affinity up to 60 times lower than the respective Y-DOTA, Lu-DOTA, or In-DOTA compounds. Interestingly, however, substitution of DOTA by the NODAGA chelator was able to increase massively its binding affinity in contrast to the Ga-DOTA analog. The 3 NODAGA analogs are antagonists in functional tests. In vivo biodistribution studies comparing ^{68}Ga-DOTATATE agonist with ^{68}Ga-DOTA-JR11 and ^{68}Ga-NODAGA-JR11 showed not only that the JR11 antagonist radioligands were superior to the agonist ligands but also that ^{68}Ga-NODAGA-JR11 was the tracer of choice and preferable to ^{68}Ga-DOTA-JR11 in transplantable HEK293-hsst_2 tumors in mice. One may therefore generalize that somatostatin receptor 2 antagonists are sensitive to radiometal modifications and may preferably be coupled with a ^{68}Ga-NODAGA chelator–radiometal complex.

Key Words: NODAGA chelator; neuroendocrine tumor targeting; radiometal modifications; somatostatin receptor 2 antagonists; somatostatin receptors

J Nucl Med 2012; 53:1481–1489
DOI: 10.2967/jnumed.112.102764

We demonstrated a decade ago (*1*) that somatostatin analogs may be sensitive to N-terminal radiometal modifications. For instance, Ga(III)-DOTA-OC (OC = octreotide) has a 3-fold higher affinity for somatostatin receptor 2 (sst_2) than Y(III)-DOTA-OC, Ga(III)-DOTATOC has a 6-fold higher affinity than Y(III)-DOTATOC, and Ga(III)-DOTATATE has an 8-fold higher affinity than Y(III)-DOTATATE (*1*). These improved binding affinities also translated into improved internalization rates and concomitantly higher tumor uptake (*2*). In those studies, it appeared adequate to generalize that $^{67/68}$Ga is a radiometal that systematically improved the sst_2 affinity of DOTA-conjugated somatostatin agonists and their pharmacokinetics. It was further confirmed in vivo in patients with neuroendocrine tumors that ^{68}Ga-DOTANOC, ^{68}Ga-DOTATOC, or ^{68}Ga-DOTATATE was a better imaging agent than the ^{111}In-DOTA congeners (*2–8*).

It has recently been shown that potent somatostatin receptor antagonists, known to poorly internalize into tumor cells, can visualize tumors in vivo as well as or even better than the corresponding agonists (*9*). This unexpected phenomenon was found both for sst_2- and for somatostatin receptor 3 (sst_3)-selective somatostatin analogs and may be due to the binding of the antagonist to a larger number of sites and to its slower dissociation rate. A pilot clinical trial with radiolabeled DOTA-linked sst_2 antagonists recently confirmed the animal data (*10*). More potent sst_2 antagonists aiming at that same purpose have been developed (*11*). To achieve this goal, several functional tests able to distinguish an agonist from an antagonist had to be developed (*11,12*).

In the light of these recent developments, it was therefore a logical consequence to investigate whether somatostatin antagonists were maintaining the same sensitivity to N-terminal modifications. We therefore selected the somatostatin antagonists

Received Jan. 5, 2012; revision accepted Apr. 30, 2012.
For correspondence or reprints contact: Jean Claude Reubi, Division of Cell Biology and Experimental Cancer Research, Institute of Pathology, University of Berne, P.O. Box 62, Murtenstrasse 31, CH-3010 Berne, Switzerland.
E-mail: reubi@pathology.unibe.ch
Published online Jul. 31, 2012.

with the best affinity and highest hydrophilicity that we have recently developed (*11,13*)—such as DOTA-*p*-NO_2-Phe-c[D-Cys-Tyr-D-Aph(Cbm)-Lys-Thr-Cys]-D-Tyr-NH_2 (DOTA-JR10), DOTA-Cpa-c[D-Cys-Aph(Hor)-D-Aph(Cbm)-Lys-Thr-Cys]-D-Tyr-NH_2 (DOTA-JR11), and DOTA-*p*-Cl-Phe-c[D-Cys-Tyr-D-Aph(Cbm)-Lys-Thr-Cys]-D-Tyr-NH_2 (DOTA-LM3) (Table 1) (*11,13*)—and coupled various metal ions to these DOTA conjugates such as Y(III), In(III), Lu(III), Cu(II), and Ga(III). In some analogs, we replaced DOTA with 1,4,7-triazacyclononane,1-glutaric acid-4,7-acetic acid (NODAGA), known to be a particularly good chelator for Ga(III) and Cu(II) (*13,14*). The sst_1–sst_5 binding affinities of these compounds were determined in vitro. Selected compounds with high sst_2 affinity were tested for their biodistribution in vivo in animals bearing HEK293-hsst_2–expressing tumors. As a control agonist, the pharmacokinetics of ^{68}Ga-DOTATATE were compared with those of ^{68}Ga-labeled somatostatin-based antagonists.

MATERIALS AND METHODS

Reagents and Cell Lines

All reagents were of the best grade available and were purchased from common suppliers. The ^{68}Ge/^{68}Ga-generator IGG100 was

TABLE 1
Chemical Structure and IC_{50} Values of sst_2 Antagonists Based on JR10, JR11, and LM3 Family and Their Metallated Conjugates

Code number	Chemical structure	IC_{50} (nM)				
		sst1	sst2	sst3	sst4	sst5
DOTA-JR11*	DOTA-Cpa-c[D-Cys-Aph(Hor)-D-Aph(Cbm)-Lys-Thr-Cys]-D-Tyr-NH_2	>1,000	0.72 ± 0.12	>1,000	>1,000	>1,000
Ga-DOTA-JR11	[^{nat}Ga]-DOTA-Cpa-c[D-Cys-Aph(Hor)-D-Aph(Cbm)-Lys-Thr-Cys]-D-Tyr-NH_2	>1,000	29 ± 2.7	>1,000	>1,000	>1,000
Y-DOTA-JR11	[^{nat}Y]-DOTA-Cpa-c[D-Cys-Aph(Hor)-D-Aph(Cbm)-Lys-Thr-Cys]-D-Tyr-NH_2	>1,000	0.47 ± 0.05	>1,000	>1,000	>1,000
Lu-DOTA-JR11	[^{nat}Lu]-DOTA-Cpa-c[D-Cys-Aph(Hor)-D-Aph(Cbm)-Lys-Thr-Cys]-D-Tyr-NH_2	>1,000	0.73 ± 0.15	>1,000	>1,000	>1,000
Cu-DOTA-JR11	[^{nat}Cu]-DOTA-Cpa-c[D-Cys-Aph(Hor)-D-Aph(Cbm)-Lys-Thr-Cys]-D-Tyr-NH_2	>1,000	16 ± 1.2	>1,000	>1,000	>1,000
In-DOTA-JR11	[^{nat}In]-DOTA-Cpa-c[D-Cys-Aph(Hor)-D-Aph(Cbm)-Lys-Thr-Cys]-D-Tyr-NH_2	>1,000	3.8 ± 0.7	>1,000	>1,000	>1,000
NODAGA-JR11	NODAGA-Cpa-c[D-Cys-Aph(Hor)-D-Aph(Cbm)-Lys-Thr-Cys]-D-Tyr-NH_2	>1,000	4.1 ± 0.2	>1,000	>1,000	>1,000
Ga-NODAGA-JR11	[^{nat}Ga]-NODAGA-Cpa-c[D-Cys-Aph(Hor)-D-Aph(Cbm)-Lys-Thr-Cys]-D-Tyr-NH_2	>1,000	1.2 ± 0.2	>1,000	>1,000	>1,000
DOTA-JR10†	DOTA-*p*-NO_2-Phe-c[D-Cys-Tyr-D-Aph(Cbm)-Lys-Thr-Cys]-D-Tyr-NH_2	>1,000	0.62 ± 0.21	>1,000	>1,000	>1,000
Ga-DOTA-JR10	[^{nat}Ga]-DOTA-*p*-NO_2-Phe-c[D-Cys-Tyr-D-Aph(Cbm)-Lys-Thr-Cys]-D-Tyr-NH_2	>1,000	8.9 ± 2.2	>1,000	>1,000	>1,000
In-DOTA-JR10	[^{nat}In]-DOTA-*p*-NO_2-Phe-c[D-Cys-Tyr-D-Aph(Cbm)-Lys-Thr-Cys]-D-Tyr-NH_2	>1,000	2.3 ± 0.5	>1,000	>1,000	>1,000
Lu-DOTA-JR10	[^{nat}Lu]-DOTA-*p*-NO_2-Phe-c[D-Cys-Tyr-D-Aph(Cbm)-Lys-Thr-Cys]-D-Tyr-NH_2	>1,000	1.2 ± 0.2	>1,000	>1,000	>1,000
NODAGA-JR10	NODAGA-*p*-NO_2-Phe-c[D-Cys-Tyr-D-Aph(Cbm)-Lys-Thr-Cys]-D-Tyr-NH_2	>1,000	23.0 ± 1.5	>1,000	>1,000	>1,000
Ga-NODAGA-JR10	[^{nat}Ga]-NODAGA-*p*-NO_2-Phe-c[D-Cys-Tyr-D-Aph(Cbm)-Lys-Thr-Cys]-D-Tyr-NH_2	>1,000	6.5 ± 0.5	>1,000	>1,000	>1,000
DOTA-LM3	DOTA-*p*-Cl-Phe-c[D-Cys-Tyr-D-Aph(Cbm)-Lys-Thr-Cys]-D-Tyr-NH_2	>1,000	0.39 ± 0.05	>1,000	>1,000	>1,000
Ga-DOTA-LM3‡	[^{nat}Ga]-DOTA-*p*-Cl-Phe-c[D-Cys-Tyr-D-Aph(Cbm)-Lys-Thr-Cys]-D-Tyr-NH_2	>1,000	12.5 ± 4.3	>1,000	>1,000	>1,000
In-DOTA-LM3	[^{nat}In]-DOTA-*p*-Cl-Phe-c[D-Cys-Tyr-D-Aph(Cbm)-Lys-Thr-Cys]-D-Tyr-NH_2	>1,000	1.3 ± 0.1	>1,000	>1,000	>1,000
Ga-NODAGA-LM3‡	[^{nat}Ga]-NODAGA-*p*-Cl-Phe-c[D-Cys-Tyr-D-Aph(Cbm)-Lys-Thr-Cys]-D-Tyr-NH_2	>1,000	1.3 ± 0.2	>1,000	>1,000	>1,000
Reference agonist, Ga-DOTATATE§	[^{nat}Ga]-DOTA-D-Phe-c[Cys-Tyr-D-Trp-Lys-Thr-Cys]-Thr	>1,000	0.2 ± 0.04	>1,000	300 ± 140	377 ± 18

*Corresponds to peptide 31 in Cescato et al. (*11*).
†Corresponds to peptide 3 in Cescato et al. (*11*).
‡Described in Fani et al. (*13*).
§Described in Reubi et al. (*1*).
Data are expressed in nmol/L (mean ± SEM; $n \geq 3$).

available from Eckert & Ziegler. The sst_2-specific antibody R2-88 was provided by Dr. Agnes Schonbrunn. The secondary antibody Alexa Fluor 488 goat antirabbit IgG (H+L) was from Molecular Probes, Inc. Tyr^3-octreotide (TOC) was from Novartis.

The HEK293 cell line expressing the T7-epitope–tagged human sst_2 (HEK-$hsst_2$) was cultured at 37°C and 5% CO_2 in Dulbecco modified Eagle medium containing 10% fetal bovine serum, penicillin (100 U/mL), streptomycin (100 μg/mL), and G418 (500 μg/mL) (*15*). All culture reagents were from Gibco BRL, Life Technologies.

Synthesis of Analogs, Coupling to Chelators and Radiometals

The unnatural amino acids D-Aph(Cbm) (D-4-amino-Phe-carbamoyl) and Aph(Hor) (amino-Phe-hydroorotic acid) were synthesized as described earlier (*13,16*). The peptide analogs JR10, JR11, and LM3 and the corresponding DOTA and NODAGA conjugates (Table 1) were synthesized following standard solid-phase peptide synthesis on a methyl-benzhydrylamine resin as previously described (*11,13*).

The ^{nat}In, ^{nat}Y, ^{nat}Lu, ^{nat}Cu, and ^{nat}Ga complexes of the conjugates were prepared using an excess (2- up to 3.5-fold) of $^{nat}InCl_3$, $^{nat}YCl_3 \times xH_2O$, $^{nat}LuCl_3 \times 6H_2O$, $^{nat}CuCl_2 \times 2H_2O$, and $^{nat}Ga(NO_3)_3 \times H_2O$, respectively, in ammonium acetate buffer, 0.2 M, pH 5, at 95°C (30 min) or at room temperature (^{nat}Ga and ^{nat}Cu-NODAGA conjugates). Free metal ions were separated by preparative high-performance liquid chromatography (*11*), or they were eliminated by SepPak C-18 purification (Waters), in which the metallopeptides were eluted with ethanol. The fractions containing the metallopeptides were evaporated to dryness, redissolved in water, and lyophilized.

^{68}Ga-labeled DOTATATE, DOTA-JR11, and NODAGA-JR11 were prepared using the Modular-Lab PharmTracer module from Eckert & Ziegler. Briefly, the $^{68}Ge/^{68}Ga$-generator was eluted with 7 mL of HCl 0.1 N, and the eluate (~900 MBq) was loaded onto a cation exchange column (Strata-XC; Phenomenex). ^{68}Ga was eluted with 800 μL of a mixture of acetone/HCl (97.6%/0.02N) directly in a vial containing 2 mL of sodium acetate buffer (0.2 M, pH 4.0) and the minimum necessary amount of 10 μg of the conjugate. DOTATATE and DOTA-JR11 were labeled at 95°C within 8 min and NODAGA-JR11 at room temperature within 10 min, followed by SepPak C-18 purification to remove uncomplexed radiometal. The radiotracers were obtained in a radiochemical yield greater than 97% after purification and in specific activities ranging between 80 and 100 MBq/nmol. Quality control was performed by analytic high-performance liquid chromatography (*13*). The radiotracer solutions were prepared by dilution with 0.9% NaCl.

In Vitro sst_1–sst_5 Autoradiography

Receptor autoradiography was performed on 20-μm-thick cryostat (HM 500; Microm) sections of membrane pellets prepared from cell lines expressing the human sst_1–sst_5 as previously described (*1,17*). For each of the tested compounds, complete displacement experiments with the universal somatostatin radioligand ^{125}I-[Leu^8,D-Trp^{22},Tyr^{25}]-somatostatin-28 (^{125}I-LTT-SRIF-28) (74,000 MBq/mmol [2,000 Ci/mmol]; Anawa) using 15,000 cpm/100 μL and increasing concentrations of the unlabeled peptide ranging from 0.1 to 1,000 nM were performed. As a control, unlabeled SRIF-28 was run in parallel using the same increasing concentrations. The sections were incubated with ^{125}I-LTT-SRIF-28 for 2 h at room temperature in Tris-HCl buffer (170 mmol/L, pH 8.2) containing 1% bovine serum albumin, bacitracin (40 mg/L), and $MgCl_2$ (10 mmol/L) to inhibit endogenous proteases. The incubated sections were washed twice for 5 min in cold Tris-HCl (170 mmol/L, pH 8.2) containing 0.25% bovine serum albumin. After a brief dip in Tris-HCl (170 mmol/L, pH 8.2), the sections were dried quickly and exposed for 1 wk to Kodak BioMax MR film. Inhibitory concentration of 50% (IC_{50}) values were calculated after quantification of the data using a computer-assisted image processing system as described previously (*18*). Tissue standards (autoradiographic ^{125}I or ^{14}C microscales; GE Healthcare) that contained known amounts of isotope, cross-calibrated to tissue-equivalent ligand concentrations, were used for quantification (*11,19*).

In Vitro Functional Assay for Agonism or Antagonism

An immunofluorescence microscopy-based internalization assay for sst_2 was performed as previously described (*15,17*). HEK-$hsst_2$ cells were grown on 35-mm 4-well plates (Cellstar; Greiner Bio-One GmbH) coated with poly-D-lysine (20 μg/mL) (Sigma-Aldrich). To distinguish whether the tested analogs are agonists or antagonists with respect to stimulating receptor internalization, HEK-$hsst_2$ cells were treated for 30 min at 37°C in growth medium, either with vehicle alone (negative control) or with 10 nM TOC (positive control), 10 nM TOC in the presence of an excess (1 μM) of the somatostatin analogs, or 1 μM of the somatostatin analogs alone when the analogs were tested for agonism. The cells were processed for immunofluorescence microscopy and then imaged using a Leica DM RB immunofluorescence microscope and an Olympus DP10 camera.

Biodistribution in HEK-$hsst_2$–Bearing Animals

All animal experiments were performed in accordance with the guidelines for the use of living animals in scientific studies and the German Law for the protection of animals. Female athymic nude mice, 4–6 wk old, were injected subcutaneously in the right shoulder with 10^7 HEK-$hsst_2$ cells, freshly suspended in 100 μL of sterile phosphate-buffered saline. The tumors were allowed to grow for 14–18 d (tumor weight, 250–350 mg).

Mice were injected with ^{68}Ga-DOTATATE, ^{68}Ga-DOTA-JR11, or ^{68}Ga-NODAGA-JR11 (100 pmol/100 μL/~5–8 MBq) via the tail vein and were euthanized at 1 and 2 h after injection. Nonspecific uptake of all radiopeptides was determined with a coinjection of a 1,500-fold excess of the corresponding unlabeled conjugate. Organs of interest and blood were collected, rinsed of excess blood, blotted dry, weighed, and counted in a γ-counter. The results were expressed as percentage of injected activity per gram of tissue (%IA/g) and represent the mean ± SD of $n = 3$–5. The total counts injected per mouse were determined by extrapolation from counts of a known aliquot of the injected solution.

Small-Animal PET Studies

PET scans were obtained using a dedicated small-animal PET scanner (Focus 120 microPET scanner; Concorde Microsystems Inc.). ^{68}Ga-DOTATATE, ^{68}Ga-DOTA-JR11, and ^{68}Ga-NODAGA-JR11 were administered to mice with HEK-$hsst_2$ tumor xenografts, as described above. Animals were anesthetized with 1.5% isoflurane, and static scans were acquired at 1 and 2 h after injection, for 20–30 min. Blocking experiments were performed as described above, and static scans were obtained at 1 h after injection. PET images were reconstructed with filtered backprojection. No correction was applied for attenuation. Images were

generated using AMIDE software. The color scale was set from 0% to 20% to allow for qualitative comparison among the images.

Data Analysis

Statistical analysis was performed by unpaired 2-tailed *t* testing using Prism software (GraphPad Software Inc.). *P* values of less than 0.05 were considered significant.

RESULTS

Affinity Studies and Agonist or Antagonist Properties

Table 1 summarizes the IC_{50} values for all compounds using ^{125}I-LTT-SRIF-28. All analogs are highly specific for sst_2.

In the JR11 family, yttrium or indium coupling to DOTA retains a high sst_2 affinity comparable to the DOTA-JR11 compound without metal. Although indium diminishes the sst_2 affinity 8-fold, copper and especially gallium induce a massive loss of the sst_2 affinity by almost 80 times. Interestingly, when DOTA is replaced by NODAGA, the effect of gallium on sst_2 affinity is completely restored, making Ga-NODAGA-JR11 a promising radiotracer (Table 1).

In the JR10 family, the same tendency of lowering the sst_2 affinity by coupling gallium to DOTA is observed, when compared with indium or lutetium coupling. The sst_2 affinity is, however, improved in the Ga-NODAGA-JR10 analog (Table 1).

In the LM3 family finally, a further impressive example of the loss of sst_2 affinity of Ga-DOTA compared with In-DOTA is observed. Here again, replacing DOTA by NODAGA massively improves the affinity of the Ga-coupled analog and makes it adequate for clinical applications (Table 1).

Two examples of competition experiments with JR11 (Fig. 1) and LM3 (Fig. 2) analogs (presently the most promising somatostatin antagonist radioligands) are presented to demonstrate the different binding affinities of gallium-coupled analogs with DOTA or NODAGA, as compared with reference compounds.

Receptor internalization assays are a suitable method to characterize receptor ligands for their functional behavior. Therefore, we have used an immunofluorescence microscopy–based internalization assay to analyze the Ga-NODAGA analogs for their ability to either stimulate sst_2 internalization in HEK-hsst$_2$ cells or antagonize the agonistic effect of TOC to stimulate sst_2 internalization. Figure 3 shows that all 3 analogs are antagonists because alone at a concentration of 1 μM they are not able to stimulate sst_2 internalization but they efficiently antagonize the agonistic TOC effect at a concentration of 1 μM.

In Vivo Biodistribution Results

^{68}Ga-DOTATATE, ^{68}Ga-DOTA-JR11, and ^{68}Ga-NODAGA-JR11 biodistributions were compared at 1 and 2 h after injection. The data are reported in Tables 2–4. The radiotracers accumulated in the tumor, kidneys, and sst_2-positive organs, such as the stomach and pancreas. The 2 antagonists, ^{68}Ga-DOTA-JR11 and ^{68}Ga-NODAGA-JR11, showed significantly higher tumor uptake (23.8 ± 3.7 and 30.7 ± 1.6 %IA/g, respectively, at 1 h after injection) than did the agonist ^{68}Ga-DOTATATE (17.8 ± 2.2 %IA/g, $P < 0.05$). However, significantly higher accumulation of radioactivity in the kidneys was also found for ^{68}Ga-DOTA-JR11 and ^{68}Ga-NODAGA-JR11 (12.7 ± 3.5 and 10.4 ± 1.4 %IA/g, respectively) than for ^{68}Ga-DOTATATE (5.2 ± 0.9 %IA/g, $P < 0.05$). The uptake in the sst_2-positive organs was at the same level for ^{68}Ga-DOTATATE and ^{68}Ga-NODAGA-JR11 (e.g., stomach: 8.6 ± 1.9 and 9.9 ± 2.5 %IA/g, respectively, and pancreas: 10.8 ± 1.7 and 11.4 ± 3.6 %IA/g, respectively, $P > 0.05$), whereas significantly lower values were found for ^{68}Ga-DOTA-JR11 (stomach: 0.5 ± 0.1 %IA/g, and pancreas: 0.5 ± 0.1%IA/g, respectively, $P < 0.05$). Blocking experiments confirm the receptor-mediated uptake in the tumor and sst2-positive organs of all 3 radiotracers. Tumor uptake remained essentially the same from 1 to 2 h after injection for all 3 radiotracers. However, the antagonist ^{68}Ga-NODAGA-JR11 washed out from the sst_2-positive organs more quickly than the agonist ^{68}Ga-DOTATATE: two thirds of ^{68}Ga-NODAGA-JR11 was washed out from the stomach and pancreas after 2 h, as compared with only one third of ^{68}Ga-DOTATATE. Among all 3 radiotracers, tumor–to–non-tumor ratios were in favor of ^{68}Ga-NODAGA-JR11.

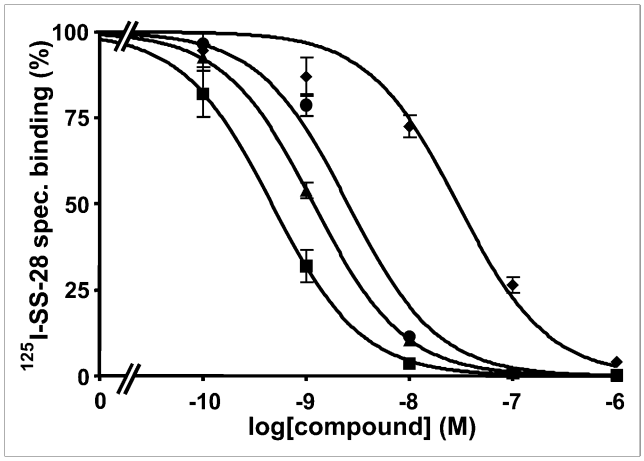

FIGURE 1. Competition experiments with cell membrane pellets of CCL39 cells expressing human sst_2, using ^{125}I-LTT-SRIF-28 as radioligand in presence of increasing concentrations of Ga-NODAGA-JR11 (▲), Y-DOTA-JR11 (■), Ga-DOTA-JR11 (♦), SRIF-28 (●) (as reference compound). spec = specific.

Small-Animal PET Images

The PET images of ^{68}Ga-DOTATATE, ^{68}Ga-DOTA-JR11, and ^{68}Ga-NODAGA-JR11 in Figure 4, reflecting the biodistribution results, illustrate not only the higher tumor uptake of the antagonists than the agonists but also the higher kidney uptake at 1 and 2 h after injection. Tumor-to-background contrast is better at 2 h after injection, especially for the antagonists. Because tumor blocking was demonstrated, the PET images of all radiotracers confirmed their specificity.

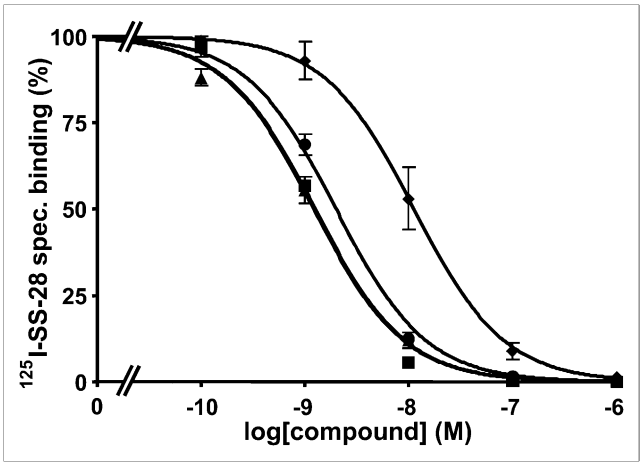

FIGURE 2. Competition experiments with cell membrane pellets of CCL39 cells expressing human sst_2, using ^{125}I-LTT-SRIF-28 as radioligand in presence of increasing concentrations of Ga-NODAGA-LM3 (▲), In-DOTA-LM3 (■), Ga-DOTA-LM3 (♦), and SRIF-28 (●) (as reference compound). spec = specific.

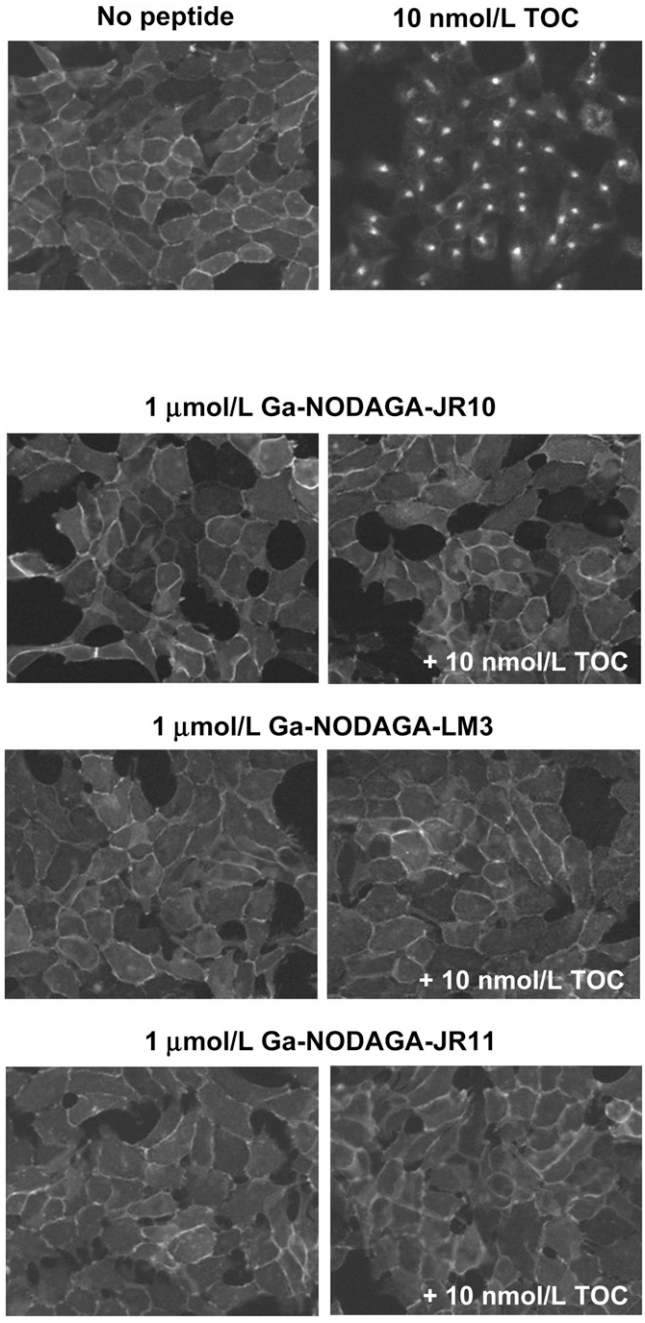

FIGURE 3. Internalization assay based on sst_2 immunofluorescence microscopy to determine whether Ga-NODAGA-JR10, Ga-NODAGA-LM3, and Ga-NODAGA-JR11 are agonists or antagonists. HEK-$hsst_2$ cells were treated either with vehicle (no peptide) or with TOC (10 nM; positive control). To test for agonism or antagonism, cells were incubated either with 1 μM of the 3 Ga-NODAGA analogs alone (left column) or with 1 μM of the 3 Ga-NODAGA analogs in presence of TOC (10 nM). After incubation with peptides, cells were processed for immunocytochemistry as described in "Materials and Methods" section. All 3 Ga-NODAGA analogs act as antagonists because given alone they are not able to stimulate sst_2 internalization, but they efficiently antagonize TOC-induced sst_2 internalization.

DISCUSSION

In the past decade, several reports have shown that adding a radiometal to a chelator–somatostatin–peptide complex had the potential to alter its receptor binding affinity or receptor subtype selectivity (*1,2*). Indeed, metallated M(III)-DOTA-octapeptide agonists targeting sst_2 show pharmacologic differences for different M(III) radiometals of high relevance in nuclear oncology. In particular, in a broad family of different octapeptides the $^{67/68}$Ga-DOTA-octapeptides performed better than the ^{111}In-, ^{90}Y-, and ^{177}Lu-DOTA-octapeptides in regard to sst_2 affinity, rate of internalization, and tumor uptake (*1,2*). These earlier preclinical studies were translated into the clinic successfully, and several ^{68}Ga-labeled peptides such as ^{68}Ga-DOTATOC, ^{68}Ga-DOTATATE, and ^{68}Ga-DOTANOC are being used in the localization of neuroendocrine tumors worldwide. All these peptide structures have full agonistic properties.

We have recently shown that radiolabeled somatostatin-based antagonists targeting sst_2 and sst_3 are superior to the above-mentioned agonists if labeled with the γ-emitter ^{111}In (*9*). The long-term goal is therefore to develop antagonist-based imaging agents for SPECT/CT and PET/CT and agents for targeted radionuclide therapy of neuroendocrine tumors.

In the in vitro part of the present study, all metallated DOTA- and NODAGA-conjugated somatostatin analogs of JR10, JR11, and LM3 (*11,13*) were shown to be of high affinity and high sst_2 selectivity and were confirmed to have antagonistic properties. Several important conclusions can be drawn from these studies: first, a clear trend for a distinct affinity influence of the radiometal was observed using the sst_2-selective DOTA-coupled antagonists of JR10, JR11, and LM3. Whereas DOTA agonists showed higher affinity when complexed to Ga(III) than to indium, yttrium, or lutetium, the inverse was found for the antagonists. Second, there is an 8-fold difference between In-DOTA-JR11 (IC_{50}, 3.8 ± 0.7 nM) and Y-DOTA-JR11 (IC_{50}, 0.47 ± 0.05 nM), indicating that ^{111}In may not be a suitable surrogate of

TABLE 2
Biodistribution Results of ^{68}Ga-DOTATATE in Nude Mice Bearing HEK-hsst$_2$ Tumor Xenografts

Organ	1 h	1-h blocking*	2 h
Blood	0.4 ± 0.0	0.8 ± 0.1	0.3 ± 0.0
Heart	0.2 ± 0.0	0.3 ± 0.0	0.2 ± 0.0
Liver	0.4 ± 0.2	0.5 ± 0.1	0.3 ± 0.0
Spleen	0.540.2	0.4 ± 0.0	0.4 ± 0.1
Lung	2.4 ± 0.7	0.8 ± 0.0	2.4 ± 0.4
Kidney	5.2 ± 0.9	7.3 ± 1.6	4.7 ± 0.9
Stomach	8.6 ± 1.9	0.5 ± 0.1	5.5 ± 0.6
Intestine	0.8 ± 0.1	0.4 ± 0.2	1.00 ± 0.1
Adrenal	2.8 ± 0.5	0.6 ± 0.1	3.6 ± 1.0
Pancreas	10.8 ± 1.7	0.4 ± 0.1	7.2 ± 1.8
Muscle	0.4 ± 0.0	0.3 ± 0.1	0.4 ± 0.2
Bone	0.7 ± 0.3	0.5 ± 0.1	1.1 ± 0.5
Tumor	17.8 ± 2.2	2.2 ± 0.4	18.5 ± 5.8
Tumor–to–normal tissue ratios			
Tumor to blood	40.4		66.2
Tumor to liver	41.3		61.8
Tumor to kidney	3.4		4.0
Tumor to muscles	50.8		42.1

*Coinjection with 1,500-fold excess of DOTATATE.
Data are %IA/g ± SD, n = 3–5.

^{90}Y and therefore not reliable for dosimetric studies of the therapeutic radiopeptide. Third, another striking finding from these studies is the comparison between ^{68}Ga-DOTATATE and ^{68}Ga-DOTA-JR11 illustrating the great potential of the antagonists. ^{68}Ga-DOTATATE (IC_{50}, 0.2 ± 0.04 nM) has the highest binding affinity (lowest IC_{50} value) of all radiolabeled somatostatin-based agonists whereas ^{68}Ga-DOTA-JR11 has 150-fold lower binding affinity (IC_{50}, 29 ± 2.7 nM). Looking at pharmacokinetics and tumor uptake, in particular, the low-affinity antagonist is slightly superior, which can be explained by the higher number of binding sites for antagonists versus agonists, outweighing the affinity differences. The superiority of the antagonist was also impressively demonstrated with in vitro autoradiographic studies of human tumor specimens (*20*) and also confirmed by the PET images, which show high and specific tumor uptake and an excellent background clearance already at 1 and 2 h after injection.

TABLE 3
Biodistribution Results of ^{68}Ga-DOTA-JR11 in Nude Mice Bearing HEK-hsst$_2$ Tumor Xenografts

Organ	1 h	1-h blocking*	2 h
Blood	0.6 ± 0.1	1.0 ± 0.2	0.3 ± 0.1
Heart	0.3 ± 0.1	0.5 ± 0.2	0.1 ± 0.0
Liver	0.5 ± 0.1	0.7 ± 0.2	0.3 ± 0.1
Spleen	0.5 ± 0.1	0.6 ± 0.2	0.3 ± 0.1
Lung	1.0 ± 0.2	1.8 ± 0.6	0.5 ± 0.2
Kidney	12.7 ± 3.5	14.0 ± 4.4	10.2 ± 1.6
Stomach	0.5 ± 0.1	0.7 ± 0.3	0.3 ± 0.2
Intestine	0.3 ± 0.1	0.6 ± 0.1	0.30 ± 0.2
Adrenal	2.6 ± 0.5	0.4 ± 0.1	2.4 ± 0.9
Pancreas	0.5 ± 0.1	0.3 ± 0.1	0.3 ± 0.1
Muscle	0.7 ± 0.3	0.2 ± 0.0	0.2 ± 0.1
Bone	1.4 ± 0.6	0.9 ± 0.2	1.2 ± 0.6
Tumor	23.8 ± 3.7	0.8 ± 0.2	22.4 ± 7.6
Tumor–to–normal tissue ratios			
Tumor to blood	41.1		89.5
Tumor to liver	50.7		67.8
Tumor to kidney	1.9		2.2
Tumor to muscles	33.5		106.6

*Coinjection with 1,500-fold excess of DOTA-JR11.
Data are %IA/g ± SD, n = 3–5.

TABLE 4
Biodistribution Results of ^{68}Ga-NODAGA-JR11 in Nude Mice Bearing HEK-hsst2 Tumor Xenografts

Organ	1 h	1-h blocking*	2 h
Blood	0.5 ± 0.2	1.4 ± 0.2	0.3 ± 0.2
Heart	0.3 ± 0.1	0.9 ± 0.4	0.1 ± 0.0
Liver	0.6 ± 0.1	1.2 ± 0.1	0.4 ± 0.1
Spleen	0.7 ± 0.4	1.4 ± 0.2	0.4 ± 0.0
Lung	2.7 ± 0.7	3.1 ± 0.6	0.9 ± 0.1
Kidney	10.4 ± 1.4	13.6 ± 0.3	10.5 ± 1.2
Stomach	9.9 ± 2.5	1.6 ± 0.8	3.1 ± 0.4
Intestine	0.7 ± 0.2	1.0 ± 0.5	0.4 ± 0.1
Adrenal	1.5 ± 0.4	Not determined	1.6 ± 0.2
Pancreas	11.4 ± 3.6	0.5 ± 0.0	3.8 ± 0.3
Muscle	0.2 ± 0.0	0.7 ± 0.2	0.2 ± 0.1
Bone	0.8 ± 0.1	1.1 ± 0.1	0.7 ± 0.2
Tumor	30.7 ± 1.6	2.5 ± 0.0	31.6 ± 3.5
Tumor-to-normal tissue ratios			
Tumor to blood	57.9		105.2
Tumor to liver	49.5		80.9
Tumor to kidney	3.0		3.0
Tumor to muscles	153.5		166.1

*Coinjection with 1,500-fold excess of NODAGA-JR11.
Data are %IA/g ± SD, n = 3–5.

We do not have a full explanation for the strong influence of the choice of radiometal. We explained the metal ion–dependent differences in the case of the agonists with differences in the coordination sphere as revealed by x-ray crystal structures of the model peptides Y-DOTA-D-Phe-NH_2, Ga-DOTA-D-Phe-NH_2 and Ga(NODASA) (*21,22*). X-ray structures are given in the supplemental information (supplemental materials are available online only at http://jnm.snmjournals.org). Y-DOTA-D-Phe-NH_2 has an 8-fold coordination including the amide carboxy oxygen embedding the Y(III) inside the DOTA-monoamide cage. On the contrary, in Ga-DOTA-D-Phe-NH_2, Ga(III) is hexacoordinated with a pseudooctahedral *cis* geometry, affording a free carboxymethyl group and a carboxymethylamide spacer. This keeps the pharmacophoric peptide at a distance from the chelate (*21*) and may allow higher flexibility of the cyclic peptide and therefore higher receptor binding affinity. Structural differences between Y-DOTATOC and Ga-DOTATOC were also confirmed by ^{1}H and ^{13}C NMR studies in solution (*23*).

Why the same metal coordination has a converse effect in the case of the chelate–antagonists is not clear. One can hypothesize that the spacer effect is also instrumental for the antagonists but toward lowering the affinity. This conclusion can be reached from the affinity of Cu-DOTA-JR11, which is also low (IC_{50}, 16 ± 1.2 nM), and the coordination chemistry of Cu(II)-DOTA, which is similar to that of Ga(III)-DOTA. The geometry is pseudooctahedral and hexacoordinate, and one can strongly assume that in solution the carboxymethyl amide function is acting as a spacer (*24–26*).

The 8-fold affinity difference between In-DOTA-JR11 and Y-DOTA-JR11 is remarkable, but again an explanation is lacking. Both metal ions, In(III) and Y(III), have spheric symmetry and differ in the ionic radius (92 pm for In(III), 101.9 pm for Y(III), both for complexes of coordination number 8). We have recently also solved the x-ray crystal structure of In-DOTA-D-Phe-NH_2 and found octacoordination. In-DOTA-D-Phe-NH_2 crystallizes as the minor diaste-

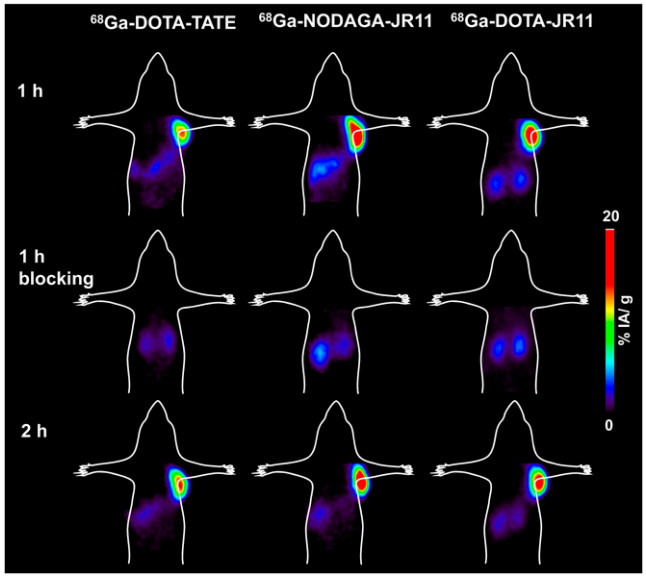

FIGURE 4. Small-animal PET images (coronal sections) of mice bearing HEK-hsst$_2$ tumor injected with ^{68}Ga-DOTATATE, ^{68}Ga-DOTA-JR11, and ^{68}Ga-NODAGA-JR11 (100 pmol/~5–8 MBq) 1 and 2 h after injection show potentiality of radioantagonists to image sst$_2$-expressing tumors in vivo. Images also illustrate higher tumor uptake of radioantagonists than agonists, and they confirm specificity of all radiotracers because no tumor is visualized in blocking experiments.

reoisomer, whereas Y-DOTA-D-Phe-NH_2 adopts the major isomer conformation. More insight into differences is brought by ^{1}H NMR studies in aqueous solution. They support octacoordination, but due to the smaller size of In(III) there is much more fluxionality within the In-DOTA-D-Phe-NH_2 cage, which again may influence the binding affinity (Heppeler et al., unpublished data).

Because the relatively high IC_{50} values of 29, 8.9, and 12.5 nM for Ga-DOTA-JR11, Ga-DOTA-JR10, and Ga-DOTA-LM3, respectively, may affect the quality of images in vivo, we searched for alternative Ga(III) chelators such as NODAGA to determine whether a chelator–Ga complex would restore a higher binding affinity. Even though the NODAGA–peptide complex may have a decreased sst_2 affinity, compared with the DOTA peptides, adding Ga^{3+} did indeed restore a high-affinity binding that is the basis of an improved in vivo tumor uptake. If we compare the sst_2 affinity of Ga-DOTATOC (IC_{50}, 2.5 ± 0.5 nmol/L) with Ga-NODAGA-TOC (IC_{50}, 3.5 ± 1.6 nmol/L) (*14*), we find no significant difference between the 2 metallopeptides.

Moreover, the biodistribution experiments showed that the antagonists Ga-DOTA-JR11 and Ga-NODAGA-JR11 are better tracers than the agonist ^{68}Ga-DOTATATE. ^{68}Ga-DOTA-JR11, having a dramatically lower affinity for the sst_2 (~150-fold) than does ^{68}Ga-DOTATATE, showed a 1.3-fold higher tumor uptake, whereas ^{68}Ga-NODAGA-JR11, with a 6-fold lower affinity, showed a tumor uptake up to 1.7-fold higher. On the contrary, the tumor uptake in the sst_2-positive organs was higher for ^{68}Ga-DOTATATE and ^{68}Ga-NODAGA-JR11 than for ^{68}Ga-DOTA-JR11, reflecting somehow their higher affinities. The IC_{50} values, which reflect the affinity of the radiotracer for the corresponding receptors, are definitively a clear indication for its in vivo uptake in the sst_2-positive tissues. However, this value is probably more predictive for the in vivo uptake in a well-organized, physiologic system expressing the receptors, such as the sst-positive normal tissues, rather than in a more disrupted system, such as the tumor environment. High target density, high association rate, and increased regional blood supply by pathologic tumor vessels may play an important role in the uptake and retention of the radiotracer in the tumor. On the other hand, a distinctly faster washout from the sst_2-positive organs was found for ^{68}Ga-NODAGA-JR11 than for ^{68}Ga-DOTATATE, whereas tumor uptake remained essentially the same. Therefore, tumor-to-background ratio is higher for ^{68}Ga-NODAGA-JR11 than for ^{68}Ga-DOTATATE over time, with the exception of the tumor-to-kidney ratio. It is, however, worth mentioning that in the case of diagnostic radiotracers the kidney uptake is not as serious a drawback as in the case of therapeutic radiopharmaceuticals. Tumor-to-blood and tumor-to-muscle are 2 relevant ratios allowing increased image contrast—ratios that are persistently much higher for the ^{68}Ga-NODAGA-JR11 over time. Additionally, an improvement on the tumor-to-liver ratio can be achieved with ^{68}Ga-NODAGA-JR11 versus ^{68}Ga-DOTATATE at 2 h. This ratio is important for sensitivity and accuracy in the diagnosis and staging of neuroendocrine tumors because often the liver is the primary site of metastasis for most of these tumors.

CONCLUSION

In this study, we demonstrated that complexation with distinct radiometals or replacing the chelator or chelate of a given peptide antagonist may dramatically affect the affinity and the in vivo profile of the radiotracer. Additionally, we showed that the radiolabeled antagonists, in particular if the chelator is NODAGA as in ^{68}Ga-NODAGA-JR11, have higher tumor uptake than the agonists, even when the affinity of the antagonist is lower by orders of magnitude. Even though ^{68}Ga-DOTATATE is a clinically accepted tracer to localize neuroendocrine tumors and is the preferred PET radiopharmaceutical in most laboratories with interest in this tumor entity, we argue that in the future ^{68}Ga-NODAGA-JR11 or equally improved antagonists should be selected for this purpose. Whether antagonists labeled with therapeutic radionuclides, for example, ^{177}Lu-DOTA-JR11, may represent a targeted vector for internal radiotherapy needs to be shown in clinical studies that we have started recently.

DISCLOSURE STATEMENT

The costs of publication of this article were defrayed in part by the payment of page charges. Therefore, and solely to indicate this fact, this article is hereby marked "advertisement" in accordance with 18 USC section 1734.

ACKNOWLEDGMENT

No potential conflict of interest relevant to this article was reported.

REFERENCES

1. Reubi JC, Schaer JC, Waser B, et al. Affinity profiles for human somatostatin receptor sst1-sst5 of somatostatin radiotracers selected for scintigraphic and radiotherapeutic use. *Eur J Nucl Med.* 2000;27:273–282.
2. Antunes P, Ginj M, Zhang H, et al. Are radiogallium-labelled DOTA-conjugated somatostatin analogues superior to those labelled with other radiometals? *Eur J Nucl Med Mol Imaging.* 2007;34:982–993.
3. Gabriel M, Decristoforo C, Kendler D, et al. ^{68}Ga-DOTA-Tyr3-octreotide PET in neuroendocrine tumors: comparison with somatostatin receptor scintigraphy and CT. *J Nucl Med.* 2007;48:508–518.
4. Srirajaskanthan R, Kayani I, Quigley AM, Soh J, Caplin ME, Bomanji J. The role of ^{68}Ga-DOTATATE PET in patients with neuroendocrine tumors and negative or equivocal findings on ^{111}In-DTPA-octreotide scintigraphy. *J Nucl Med.* 2010;51:875–882.
5. Campana D, Ambrosini V, Pezzilli R, et al. Standardized uptake values of ^{68}Ga-DOTANOC PET: a promising prognostic tool in neuroendocrine tumors. *J Nucl Med.* 2010;51:353–359.
6. Ambrosini V, Campana D, Bodei L, et al. ^{68}Ga-DOTANOC PET/CT clinical impact in patients with neuroendocrine tumors. *J Nucl Med.* 2010;51:669–673.
7. Kowalski J, Henze M, Schuhmacher J, Macke HR, Hofmann M, Haberkorn U. Evaluation of positron emission tomography imaging using [^{68}Ga]-DOTA-D Phe (1)-Tyr(3)-Octreotide in comparison to [^{111}In]-DTPAOC SPECT: first results in patients with neuroendocrine tumors. *Mol Imaging Biol.* 2003;5:42–48.
8. Hofmann M, Maecke H, Borner R, et al. Biokinetics and imaging with the somatostatin receptor PET radioligand ^{68}Ga-DOTATOC: preliminary data. *Eur J Nucl Med.* 2001;28:1751–1757.
9. Ginj M, Zhang H, Waser B, et al. Radiolabeled somatostatin receptor antagonists are preferable to agonists for in vivo peptide receptor targeting of tumors. *Proc Natl Acad Sci USA.* 2006;103:16436–16441.

10. Wild D, Fani M, Behe M, et al. First clinical evaluation of somatostatin receptor antagonist imaging [abstract]. *J Nucl Med.* 2010;51(suppl 2):483.
11. Cescato R, Erchegyi J, Waser B, et al. Design and in vitro characterization of highly sst2-selective somatostatin antagonists suitable for radiotargeting. *J Med Chem.* 2008;51:4030–4037.
12. Cescato R, Loesch KA, Waser B, et al. Agonist biased signaling at the sst2A receptor: the pan-somatostatin analogs KE108 and SOM230 activate and antagonize distinct signaling pathways. *Mol Endocrinol.* 2010;24:240–249.
13. Fani M, Del Pozzo L, Abiraj K, et al. PET of somatostatin receptor-positive tumors using ^{64}Cu- and ^{68}Ga-somatostatin antagonists: the chelate makes the difference. *J Nucl Med.* 2011;52:1110–1118.
14. Eisenwiener KP, Prata MI, Buschmann I, et al. NODAGATOC, a new chelator-coupled somatostatin analogue labeled with [67/^{68}Ga] and [^{111}In] for SPECT, PET, and targeted therapeutic applications of somatostatin receptor (hsst2) expressing tumors. *Bioconjug Chem.* 2002;13:530–541.
15. Cescato R, Schulz S, Waser B, et al. Internalization of sst2, sst3 and sst5 receptors: effects of somatostatin agonists and antagonists. *J Nucl Med.* 2006;47:502–511.
16. Jiang G, Stalewski J, Galyean R, et al. GnRH antagonists: a new generation of long acting analogues incorporating urea functions at positions 5 and 6. *J Med Chem.* 2001;44:453–467.
17. Reubi JC, Erchegyi J, Cescato R, Waser B, Rivier JE. Switch from antagonist to agonist after addition of a DOTA chelator to a somatostatin analog. *Eur J Nucl Med Mol Imaging.* 2010;37:1551–1558.
18. Reubi JC, Kvols LK, Waser B, et al. Detection of somatostatin receptors in surgical and percutaneous needle biopsy samples of carcinoids and islet cell carcinomas. *Cancer Res.* 1990;50:5969–5977.
19. Erchegyi J, Cescato R, Grace CR, et al. Novel, potent, and radio-iodinatable somatostatin receptor 1 (sst1) selective analogues. *J Med Chem.* 2009;52:2733–2746.
20. Cescato R, Waser B, Fani M, Reubi JC. Evaluation of ^{177}Lu-DOTA-sst2 antagonist versus ^{177}Lu-DOTA-sst2 agonist binding in human cancers in vitro. *J Nucl Med.* 2011;52:1886–1890.
21. Heppeler A, Froidevaux S, Mäcke HR, et al. Radiometal-labelled macrocyclic chelator-derivatised somatostatin analogue with superb tumour-targeting properties and potential for receptor-mediated internal radiotherapy. *Chem Eur J.* 1999;5:1974–1981.
22. André JP, Maecke HR, Zehnder M, Macko L, Akyel KG. 1,4,7-Triazacyclononane-1-succinic acid-4,7-diacetic acid (NODASA): a new bifunctional chelator for radio gallium-labelling of biomolecules. *Chem Commun (Camb).* 1998;12:1301–1302.
23. Deshmukh MV, Voll G, Kuhlewein A, et al. NMR studies reveal structural differences between the gallium and yttrium complexes of DOTA-D-Phe1-Tyr3-octreotide. *J Med Chem.* 2005;48:1506–1514.
24. Riesen A, Zehnder M, Kaden TA. Metal complexes of macrocyclic ligands. Part XXIII. Synthesis, properties, and structures of mononuclear complexes with 12- and 14-membered tetraazamacrocycle-N,N′,N″,N‴-tetraacetic acids. *Helv Chim Acta.* 1986;69:2067–2073.
25. Viola NA, Rarig RS Jr, Ouellette W, Doyle RP. Synthesis, structure and thermal analysis of the gallium complex of 1,4,7,10-tetraazacyclo-dodecane-N,N′,N″,N‴-tetraacetic acid (DOTA). *Polyhedron.* 2006;25:3457–3462.
26. Heppeler A, André JP, Buschmann I, et al. Metal-ion-dependent biological properties of a chelator-derived somatostatin analogue for tumour targeting. *Chemistry.* 2008;14:3026–3034.